A STUDY OF FORCED CONVECTION WITHIN A HORIZONTAL CAVITY WITH EIGHTEEN STATIONARY HEATED CYLINDERS

Paulo Mohallem Guimarães , paulomgui@uol.com.br
Eduardo Miguel da Silva, m_eduardo_silva@yahoo.com.br
Rogério José da Silva, rogeriojs@unifei.edu.br
Genésio José Menon, genesio@unifei.edu.br
Universidade Federal de Itajubá – UNIFEI
Departamento de Engenharia Mecânica
Avenida BPS, 1303 – Pinheirinho – Itajubá – MG – 37500-176

Abstract. *This work analyses the forced convection in a horizontal cavity with a tube bank composed of 18 stationary cylinders. One wall is allowed to transfer heat while the remaining are insulated. The flow is induced by one fan placed near the upper horizontal wall. No buoyancy forces are considered. The finite element method is applied to solve the continuity, momentum, and energy equations using 4-node elements. Furthermore, the Petrov-Galerkin method and the penalty technique are applied to deal with difficulties in the convective and pressure terms, respectively. Numerical and experimental comparisons are also carried out to validate the code. Temperature and velocity distributions are presented showing their correlation with the Nusselt number for various Reynolds numbers. Some recirculations worked as isolations layers that made heat transfer more difficult.*

Keywords*: finite element method, cylinder, Petrov-Galerkin, convective heat transfer, laminar flow*

1. INTRODUCTION

The study of natural, mixed, and forced convection in enclosures have been carried out for decades due to their importance in engineering applications such as solar energy systems, electronic cooling equipments, heat exchangers, etc.

In Fu et al. (1994), a penalty finite-element numerical method was used to investigate enhancement of natural convection of an enclosure by a rotating circular cylinder near a hot wall. They concluded that the direction of the rotating cylinder played a role in enhancing natural convection in an enclosure. In this study, the counter-clockwise rotating cylinder apparently contributed to increase the heat transfer rate, but the clockwise rotating cylinder did not. When the value of the Richardson number is about 10^3, the enhancement of the heat transfer rate begins to be revealed. The maximum enhancement of the heat transfer is approximately equal to 60%.

Nguyen et al. (1996) investigated numerically the heat transfer from a rotating circular cylinder immersed in a spatially uniform, time-dependent convective environment including the effects of buoyancy forces. The flow equations, based on the vorticity and stream function, are solved along with the energy equation by a hybrid spectral scheme that combines the Fourier spectral method in the angular direction and a spectral element method in the radial direction. Several cases are simulated for Grashof numbers up to 2×10^4, Reynolds numbers up to 200, and a range of speed of rotation from –0.5 to +0.5. The results showed that vortex shedding was promoted by the cylinder rotation but it was vanished because of buoyancy forces. In opposing flows, the counter flow currents cause a large expansion of the streamlines and isotherms in the direction normal to the free stream velocity. These changes in the structure of the flow and the temperature fields greatly modify the heat flux along the surface of the cylinder and consequently, the heat transfer rate is strongly dependent upon Reynolds number, Grashof number, rotational speed, and the gravity direction. Effects due to pulsation are also reflected in the Nusselt number history in the form of periodic oscillations.

Lee et al. carried out experimental investigations to study the convective phenomena of an initially stratified salt-water solution due to bottom heating in a uniformly rotating cylindrical cavity. Three types of global flow patterns initially appeared depending on the effective Rayleigh number and Taylor number: stagnant flow regime, single mixed layer flow regime and multiple mixed layer flow regime. The number of layers at its initial stage and the growth height of the mixed layer decreased for the same Rayleigh number. It was ascertained in the rotating case that the fluctuation of interface between layers was weakened, the growth rate of mixed layer was retarded and the shape of interface was more regular compared to the stationary case.

Joo-Sik Yoo (1998) studied numerically the mixed convection in a horizontal concentric annulus with Prandtl number equal to 0.7. The inner cylinder was hotter than the outer cylinder. The forced flow was induced by the cold outer cylinder that rotated slowly with constant angular velocity with its axis at the center of the annulus. Investigations were made for various combinations of Rayleigh number Ra, Reynolds number Re, and ratio σ of the inner cylinder diameter to the gap width, that is, $Ra \leq 5 \times 10^4$, $Re \leq 1500$, and $0.5 \leq \sigma \leq 5$. The flow patterns could be categorized into three types according to the number of eddies: two-one- and no-eddy flows. The transitional Reynolds number between two and one-eddy flows for small Rayleigh number was not greatly affected by the geometrical parameter σ. Net circulation of fluid in the direction of cylinder's rotation is decreased as Ra was increased. As the speed of the

cylinder's rotation was increased, the points of maximum and minimum local heat fluxes at both of the inner and outer cylinders move in the same direction of cylinder's rotation for small Ra, but for high Ra the points at the inner cylinder did not always move in the same direction. Overall heat transfer at the wall was rapidly decreased, as Re approached the transitional Re between two- and one-eddy flows.

Lin and Yan (2000) conducted an experimental study through temperature measurements to investigate the thermal features induced by the interaction between the thermal buoyancy and rotation-induced Coriolis force and centrifugal force in an air-filled heated inclined cylinder rotating about its axis. Results were obtained ranging the thermal Rayleigh number, the Taylor number, the rotational Rayleigh number, and the inclined angle. The experimental data suggested that when the cylinder was stationary, the thermal buoyancy driven flow had random oscillation at small amplitude after initial transient for inclined angle smaller than 60°. Rotating the cylinder was found to destabilize the temperature field when the rotation speed was less than 30 rpm and to stabilize it when the rotation speed exceeded 30 rpm. Moreover, the distributions of time-average temperature in the Z-direction for various inclined angles became widely separate only at low rotation rates less than 60 rpm.

In this work, a forced convection study in a rectangular cavity with a set o nine non-rotating heated cylinders on the upper right corner was carried out. This particular problem could be applied to the study of heat exchangers in industrial ovens. This dimensionless study held a laminar and unsteady regime whereas some results were shown for the steady regime.

2. GEOMETRY AND BOUNDARY CONDITIONS

Figure 1 shows the geometry and the mesh used, while the boundary conditions are as follows:

$$
\begin{aligned}
&S_1: U = V = 0 \ and \ \frac{\partial \theta}{\partial X} = 0 \ or \ \frac{\partial \theta}{\partial Y} = 0 ; \\
&S_2: U = V = 0 \ and \ \theta = 0 ; \\
&S_3: U = V = 0 \ and \ \theta = 1 ; \\
&S_4: U = 1 \ and \ V = 0 \ ; \\
&S_5: U = 0 \ and \ \frac{\partial \theta}{\partial X} = 0 \ ;
\end{aligned}
\qquad (1)
$$

where U and V are the dimensionless velocity components on X and Y directions, respectively, while θ is the dimensionless temperature.

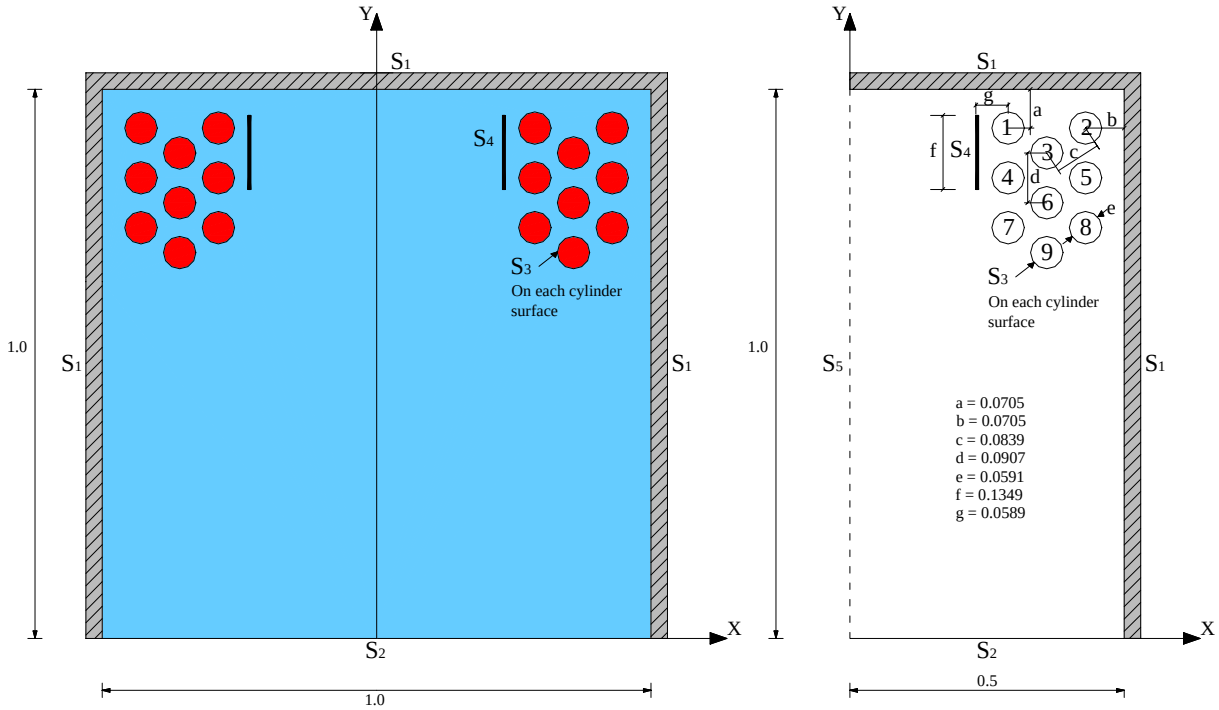

Figure 1. Geometry and boundary conditions.

Figure 2 shows only a half of the enclosure since it is symmetric in the y-direction. The domain is spatially discretized with 16448 structured and non-structured elements.

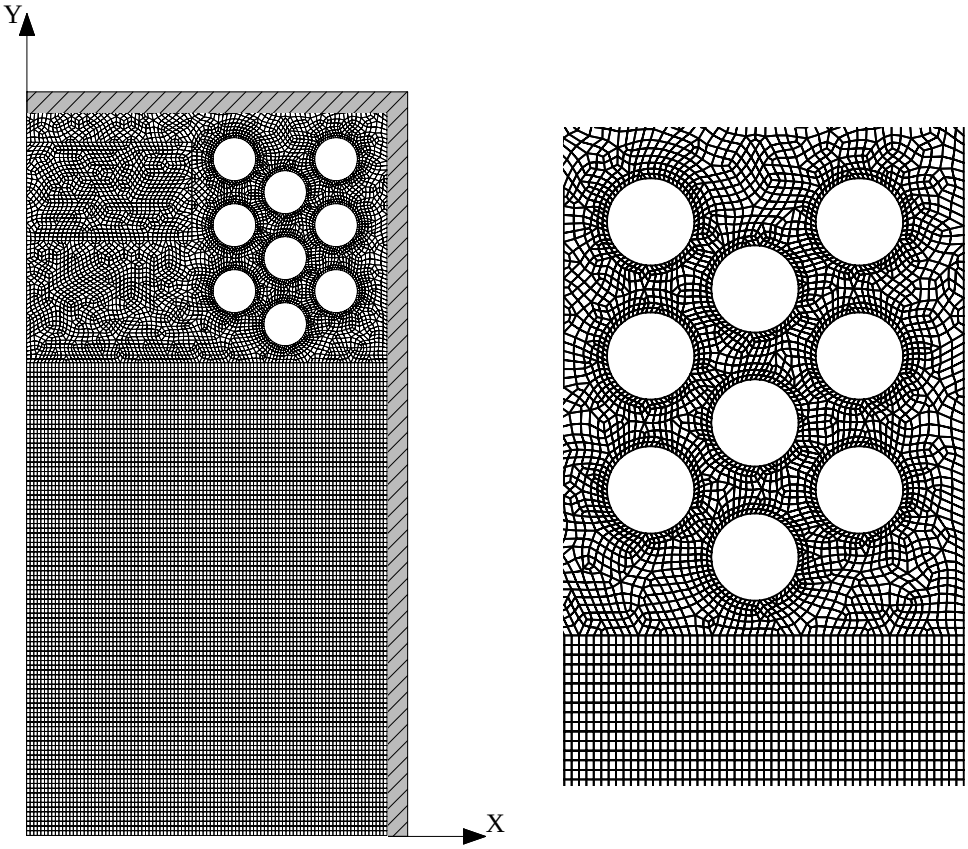

Figure 2. Mesh with 16448 structured and non-structured elements.

3. PROBLEM FORMULATION

The problem governing equations are given by the equations of mass conservation, Navier-Stokes, and energy. Applying the following dimensionless parameters:

$$X=\frac{x}{H};\quad Y=\frac{y}{H};\quad U=\frac{u}{U_0};\quad V=\frac{v}{U_0};\quad P=\frac{p}{\rho_0 U_0^2};\quad \tau=\frac{t}{\left(H/U_0\right)};\quad \theta=\left(T-T_0\right)/\Delta T\ ;\ \Delta T=T_h-T_c\ ; \tag{2}$$

$$Pr=\frac{\nu}{D_T};\qquad Re=\frac{U_0\rho_0 H}{\mu};$$

where u and v are the velocity components, T is the fluid temperature, t is the time field, D_T is the thermal diffusivity, β_T is the thermal expansion coefficient, ν is the kinematics viscosity, ρ_0 is the fluid density and T_0 is the reference temperature taken as $T_0 = T_c$, Pr is the Prandtl number, Re is the Reynolds number, U_0 is the reference velocity, and μ is the dynamic viscosity, the dimensionless governing equations can be cast into form as follows:

$$\frac{\partial U}{\partial X}+\frac{\partial V}{\partial Y}=0\ ; \tag{3}$$

$$\frac{\partial U}{\partial \tau}+U\frac{\partial U}{\partial X}+V\frac{\partial U}{\partial Y}=-\frac{\partial P}{\partial X}+\frac{1}{Re}\left(\frac{\partial^2 U}{\partial X^2}+\frac{\partial^2 U}{\partial Y^2}\right); \tag{4}$$

$$\frac{\partial V}{\partial \tau}+U\frac{\partial V}{\partial X}+V\frac{\partial V}{\partial Y}=-\frac{\partial P}{\partial Y}+\frac{1}{Re}\left(\frac{\partial^2 V}{\partial X^2}+\frac{\partial^2 V}{\partial Y^2}\right)\ ; \tag{5}$$

$$\frac{\partial \theta}{\partial \tau} + U\frac{\partial \theta}{\partial X} + V\frac{\partial \theta}{\partial Y} = \frac{1}{Re\,Pr}\left(\frac{\partial^2 \theta}{\partial X^2} + \frac{\partial^2 \theta}{\partial Y^2}\right) \quad . \tag{6}$$

The average Nusselt number along a surface S can be written as:

$$Nu = \frac{1}{S}\int_S \frac{\partial \theta}{\partial n}\, ds \,. \tag{7}$$

where n means the direction perpendicular to the surface S which can be the hot, cold, or cylinder surface.

4. THE SOLUTION METHOD

By applying the Petrov-Galerkin formulation to the equations (3) to (6) together with the Penalty technique, the weak form of the conservation equations are as follows:

$$\int_\Omega N_i\left[\frac{\partial U}{\partial t} + \frac{1}{Re}\left(\frac{\partial N_i}{\partial X}\frac{\partial U}{\partial X} + \frac{\partial N_i}{\partial Y}\frac{\partial U}{\partial Y}\right)\right]d\Omega + \int_\Omega^R \lambda\frac{\partial N_i}{\partial X}\left(\frac{\partial U}{\partial X} + \frac{\partial V}{\partial Y}\right)d\Omega = \int_\Omega \left(N_i + P_{i1}\right)\left(U\frac{\partial U}{\partial X} + V\frac{\partial U}{\partial Y}\right)d\Omega - \int_{\Gamma_0} N_i\; p\, n_x\, d\Gamma \quad ; \tag{8}$$

$$\int_\Omega N_i\left[\frac{\partial V}{\partial t} + \frac{1}{Re}\left(\frac{\partial N_i}{\partial X}\frac{\partial V}{\partial X} + \frac{\partial N_i}{\partial Y}\frac{\partial V}{\partial Y}\right)\right]d\Omega + \int_\Omega^R \lambda\frac{\partial N_i}{\partial Y}\left(\frac{\partial U}{\partial X} + \frac{\partial V}{\partial Y}\right)d\Omega = \int_\Omega \left[\left(N_i + P_{i1}\right)\left(U\frac{\partial V}{\partial X} + v\frac{\partial V}{\partial Y}\right)\right]d\Omega - \int_{\Gamma_0} N_i\; p\, n_y\, d\Gamma \quad ; \tag{9}$$

$$\int_\Omega\left[N_i\frac{\partial \theta}{\partial t} + \frac{1}{Re\,Pr}\left(\frac{\partial N_i}{\partial x}\frac{\partial \theta}{\partial x} + \frac{\partial N_i}{\partial y}\frac{\partial \theta}{\partial y}\right)\right]d\Omega = \int_\Omega \left(N_i + P_{i2}\right)\left(u\frac{\partial \theta}{\partial x} + v\frac{\partial \theta}{\partial y}\right)d\Omega + \int_{\Gamma_1} N_i\; q\, d\Gamma \,; \tag{10}$$

where $q = 0$ (no heat flux). The dependent variables are approximated by:

$$\Phi\left(X,Y,t\right) = \sum_j N_j(X,Y)\Phi_j\left(t\right)\;;\; p\left(X,Y,t\right) = \sum_k M_k(X,Y)p_k\left(t\right). \tag{11}$$

N_i and N_j denote the linear shape functions for Φ, that is, for U, V, and θ, and M_k denote the shape functions for the constant piecewise pressure. P_{ij} are the Petrov-Galerkin perturbations applied to the convective terms only. The terms P_{ij} are defined as follows:

$$P_{ij} = k_j\left(U\frac{\partial N_i}{\partial X} + V\frac{\partial N_i}{\partial Y}\right);\; k_j = \frac{\alpha_j \bar{h}}{|V|}\;;\; \alpha_j = coth\frac{\gamma_j}{2} - \frac{2}{\gamma_j}\;;\; \gamma_j = \frac{|V|\bar{h}}{\varepsilon_j}\;;\; j=1,2 \tag{12}$$

where γ is the element Péclet number, $|V|$ is the absolute value of the velocity vector that represents the fluid average velocity within each element, $\bar{h}$ is the element average size, $\varepsilon_1 = 1/Re, \varepsilon_2 = 1/Pe$, and λ is the Penalty parameter which is considered to be 10^9. The time integration is by a semi-implicit backward Euler method. Moreover, the convective terms are calculated explicitly and the viscous and Penalty terms implicitly. The temperatures and velocities are interpolated by using the four-node quadrilateral elements and the pressure by the one-node ones. Finally, the reduced integration is applied to the penalty term to avoid numerical locking. Pressures P are approximated by:

$$P = -\lambda\nabla.V\;; \tag{13}$$

and

$$\nabla.V = -\frac{P}{\lambda}\;; \tag{14}$$

Therefore, with the value of the divergent mapping, mass conservation could be checked.

5. CODE VALIDATION

The algorithm was validated by comparing the results of the present work with results obtained from experimental and numerical investigations. The first comparison was accomplished not only by using the experimental results presented by Lee and Mateescu (1998) and Armaly et al. (1983), but also by the numerical ones achieved by Lee and Mateescu (1998), Gartling (1990), Kim and Moin (1985), and Sohn (1988). The air flow of the present comparison analysis was taken as two-dimensional, laminar, incompressible, and under the unsteady regime. The domain was a horizontal upstream backward-facing step channel whose inlet had a fully developed velocity profile given by $u = 24y(0.5\text{-}y)\,\overline{U}$ and $v = 0$ in which $Re = 800$. Good agreement was found. The second comparison was performed with the numerical results from Comini et al. (1997). The contrasting study was carried out by considering a problem involving a Poiseiulle flow heated from below with velocity and temperature profiles at the inlet given by $U = 6Y(1\text{-}Y)$ and $\theta = 1\text{-}Y$, respectively. The flow was considered to be two-dimensional, laminar, and incompressible in the unsteady regime. In this case, some values were chosen such as Re=10, Pr = 0.67, and Fr = 1/150. The grid had 4000 quadrilateral four-noded elements with $\Delta x = 0.1$, $\Delta y = 0.15$ and $\Delta t = 0.01$. After approximately iteration 500, the regime turned to be quasi-periodic with the average Nusselt number on the upper wall oscillating around a mean value of 2.44. This value agreed satisfactorily with the one from Comini et al. (1997), which was 2.34, resulting in a deviation of about 4%. The third case studied to validate the mathematical modeling code was featured by mixed convection of air between two horizontal concentric cylinders with a cooled rotating outer cylinder with Pr = 0.7, Re = 10, 50, 100, 150, 200, 250, 300, 350, and 500, and Ra = 10^4, 2 x 10^4, and 5 x 10^4. The domain was discretized spatially with 5976 non-structured four-node quadrilateral elements. The results found here were higher than the ones in Yoo (1998). This difference was likely due to different methods and different meshes comparing to the ones used in Yoo (1998). The time step used was 0.01 for almost all cases and the number of iterations ranged from 10^4 to $3x10^4$.

5. RESULTS

Figure 4 shows temperature, velocity, and streamline distributions for Reynolds number Re = 100, 250, 750, and 1000. The streamlines are only shown to assure the understanding of flow directions and recirculations. For all cases, there are two opposite recirculations before the flow entrance between cylinders 1 and 4. Although the size of these two recirculations tend to decrease as Re increases, more intense velocities are present for Re = 1000. All flows are mainly governed by two big cells. Interestingly, for high Re, the cells near the cold surface do not get smaller as Re increases. The other cell velocities get much stronger as Re increases. As for the temperature, the cold fluid tends to be confined near the cold wall. However, for Re = 1000, this cold fluid tries to find its way along the right insulated wall.

Figure 5 depicts the pressure smoothed by the least square method in order to check mass conservation as it is a matter of great importance due to a penalty method has been applied throughout this study. In fact, the pressure P from the the Navier-Stokes equations are approximated by $P = -\lambda \nabla . \boldsymbol{V}$, and then the velocity divergent can be estimated by $\nabla . \boldsymbol{V} = -P / \lambda$. Hence, by checking the order of the pressure in Fig. 5 and multiplying it by 10^{-9}, one can say that mass is preserved.

Since flows through the cylinders are quite complex, Fig. 6 pictures them in more detailed views for Re = 100, 250, 500 and 1000.The recirculations in front of cylinders 1, 4, and 7 are due to the presence of stronger pressure gradients caused by flows through the cylinders originated from a main flow between cylinders 1 and 4. From this main flow, three strong ones are branched out after reaching cylinder 3. Two of them are then responsible for blocking some passages and, hence, creating those two main recirculations in front of cylinders 1, 4, and 7. One can observe that the flow is almost stagnant between cylinders 3 and 5, and 6 and 9. This may not contribute to heat transfer. The flow on the right hand side of cylinders 2, 5, and 8 is almost one-dimensional. As Re increases, the temperature distribution tends to be uniform. It seems that as Re increases, a recirculation starts after cylinder 9.

Figure 7 shows the Nusselt number behaviour in time for Re = 100, 250, 500, and 1000. The Nusselt numbers are calculated on the cold wall Nu_c, on all cylinder surfaces together Nu_c, and on each cylinder surface Nu_i, where i = 1, 2,….., 9. Cylinders 1, 3, and 4 have the highest Nu through time. It is worth observing that Nu_1 is smaller than Nu_4 for Re = 100 and 250. For higher Re, this behaviour is just the opposite. This can be explained by the ascendant flow of hot fluid around cylinder 7 which is higher as Re increases. The temperature distribution also features this behaviour due to its weaker uniformity around cylinder 1. Flow tends to be stronger through cylinders 1 and 3, and 2 and the insulated walls for higher Re.

Finally, Fig. 8 presents the average Nusselt number in the steady state regime for Re = 100, 250, 500, 750, and 1000. Again, the higher Re is, the higher Nu_1 gets. However, for Re smaller than 500, Nu_4 is higher than Nu_1. It is interesting to notice how Nu_9 decreases and how Nu_3 increases. Furthermore, it can be noticed that $Nu_{(2,5,7,8,\text{ and } 9)}$ are too small, and thus, featuring a weak heat transfer on those surfaces. Maybe, a way of enhancing it on those areas is to make wider passages in some places guaranteeing more cold fluid reaching those cylinders. The fact that those main recirculations appear near the cold wall is certainly an issue which should be worked on to enhance heat transfer. These recirculations work as isolation layers which inhibits hot fluid coming from the cylinders to reach directly the cold wall.

If this is done, maybe the temperature distribution would be uniform. If some conductive bodies are placed within the cavity, certainly new recirculations would be brought up and therefore, again, the location of those recirculations would be extremely important in the uniformity of the temperature field. Although this is a start study, it gives important results on recirculations and their influence on heat transfer. This can provide time and money savings when trying to build such devices in food industry. More studies with higher velocities are encouraged by the authors for future works.

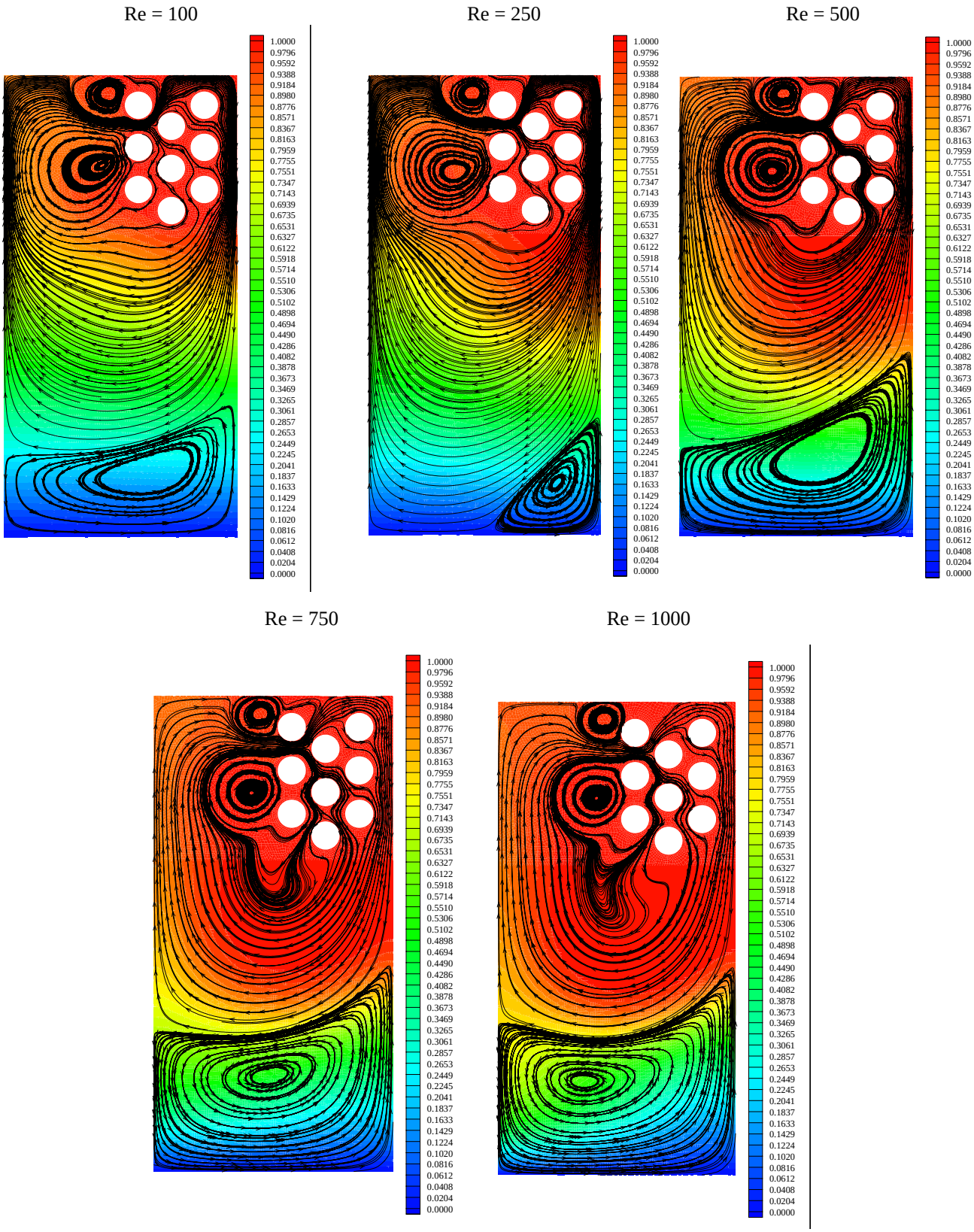

Figure 4 – Isotherms and streamlines for Re = 100, 250, 500, 750, and 1000.

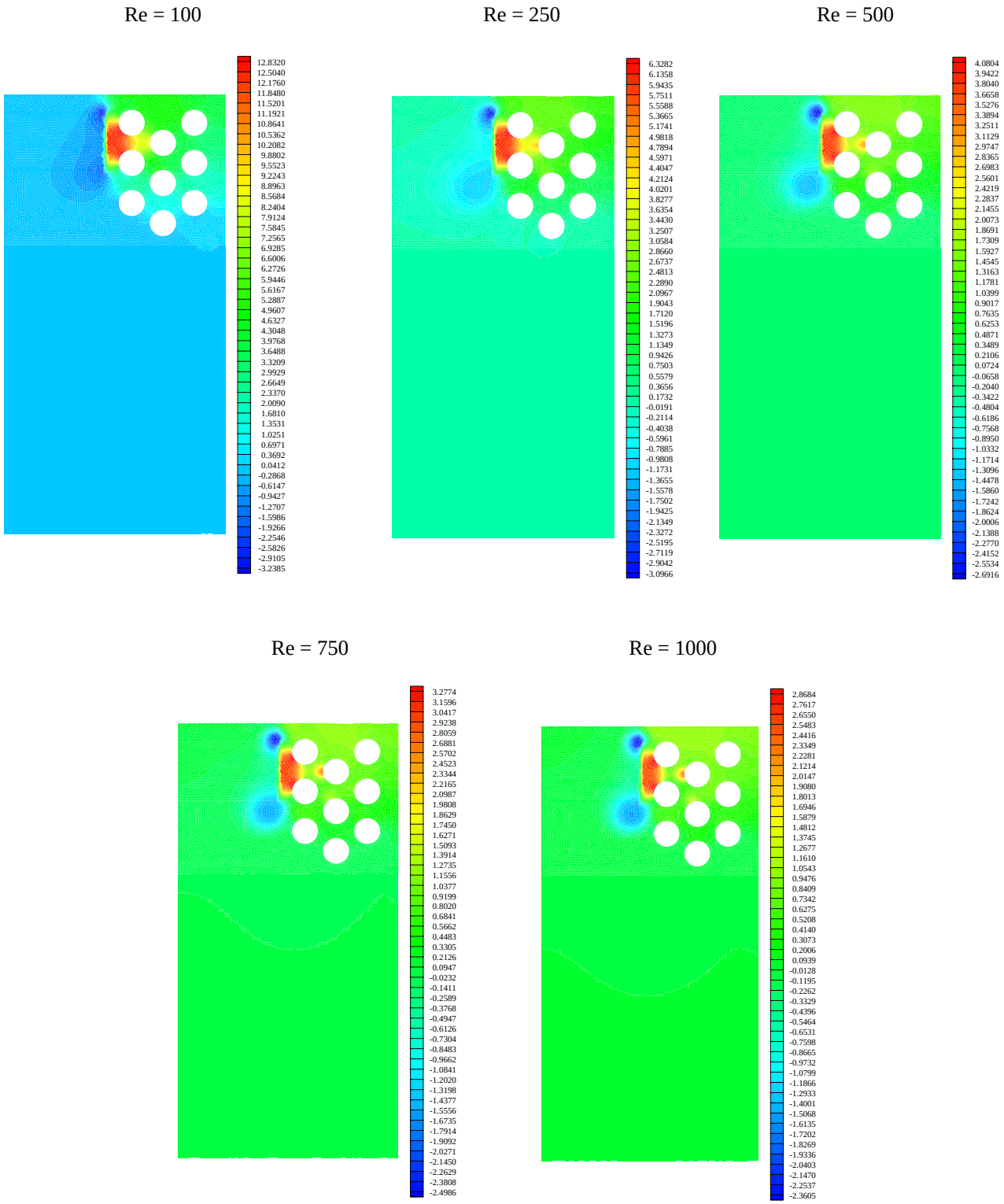

Figure 5 – Pressure field for the analysis of mass conservation.

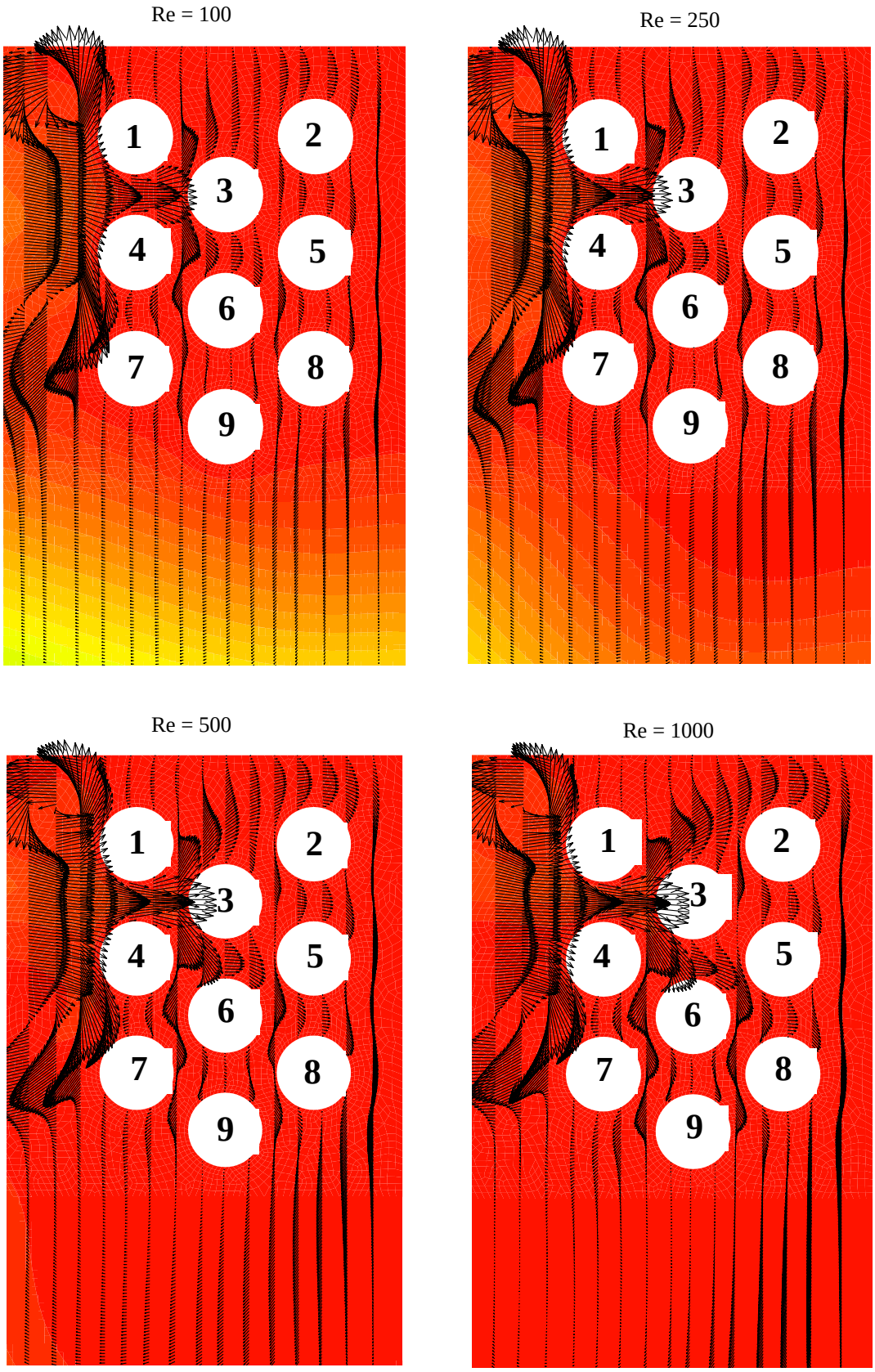

Figure 6 – Detailed view of the velocity vectors around the cylinders.

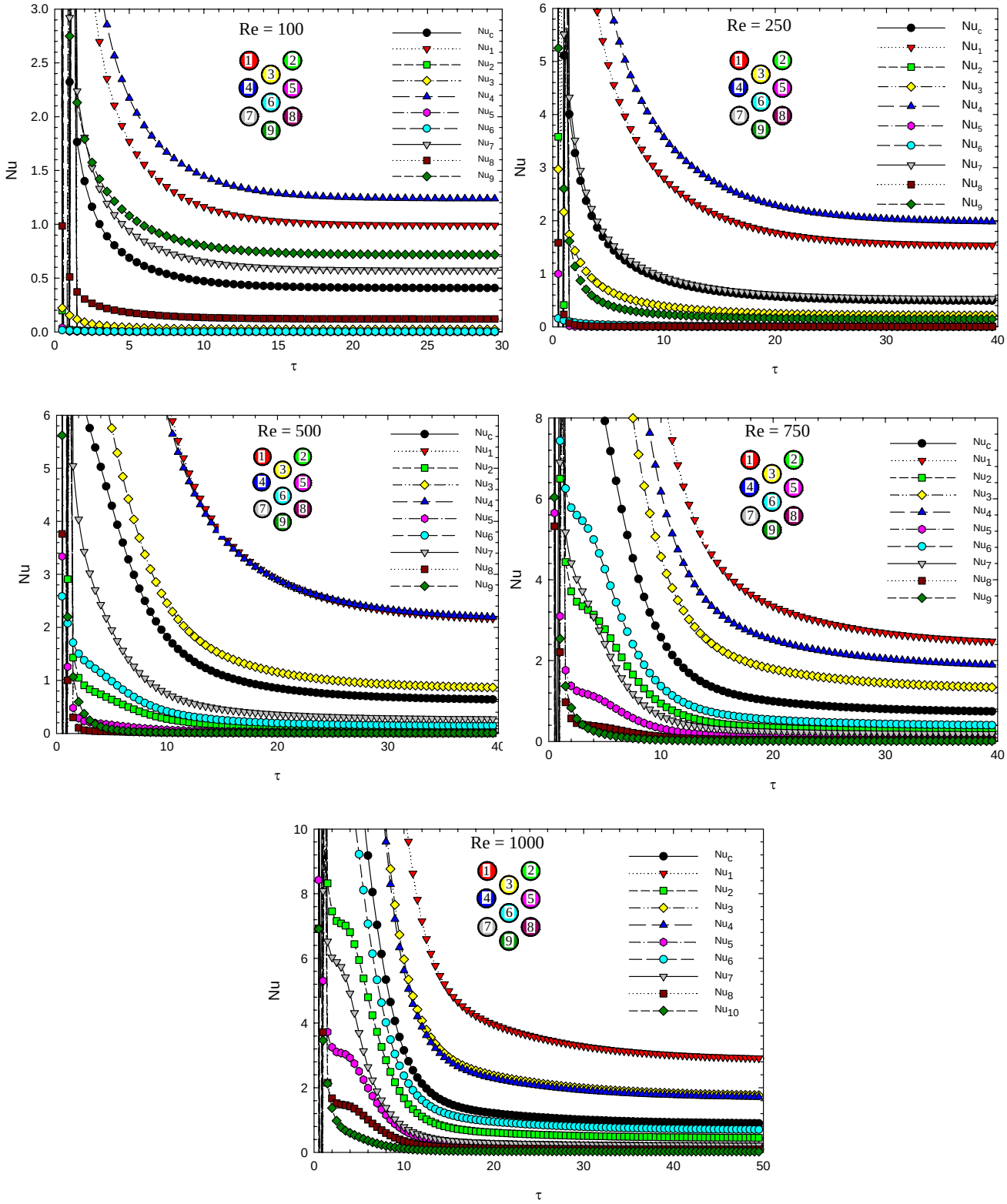

Figure 7 – Average Nusselt number versus time for Re = 100, 250, 500, 750, and 1000.

In this work, the forced convection in a cavity with three isolated walls and one cooled wall is performed featuring a start study of heat exchangers in the food field. The governing equations are numerically solved using the finite element method with the Penalty technique on the convective terms. The method makes use of linear quadrilateral elements. Some comparisons are carried out to validate the computational code developed by the authors. Flow and temperature distributions are presented and some important results are reached by varying Reynolds number from 100 to 1000.

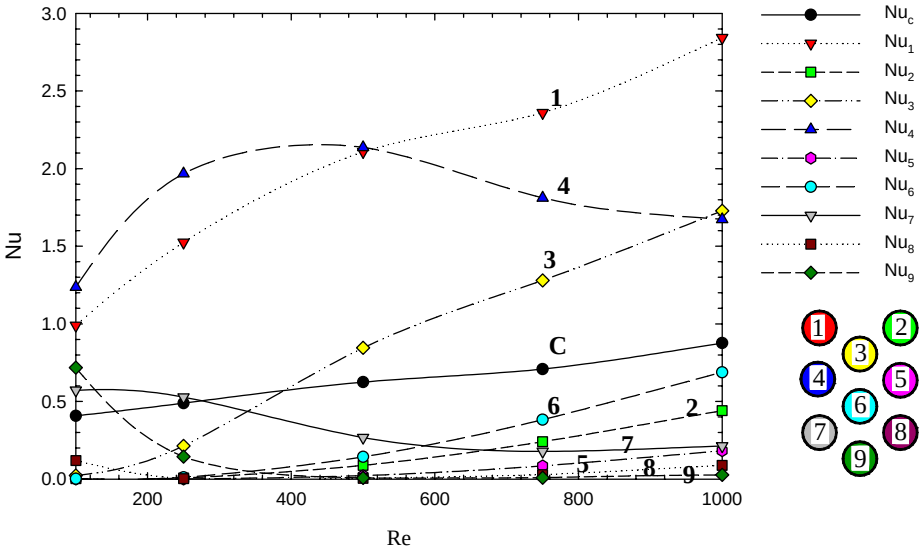

Figure 8 – Average Nusselt number for Re = 100, 250, 500, 750, and 1000.

6. CONCLUSIONS

There are some recirculations inside the cavity that are strongly correlated to the heat transfer and uniformity of temperature distribution. For all cases, a recirculation appears near the cold wall that works as an isolation layer and thus impairing heat transfer. The authors encourage some more studies in which the cylinders set configuration must be taken into account as well as higher forced velocities. Experimental studies have already been carried out by engineers from PRÁTICA TECHNOCOOK in the city of Pouso Alegre, Minas Gerais, Brazil.

7. ACKNOWLEDGEMENTS

The authors acknowledge CAPES and PRÁTICA TECHNOCOOK for the financial support without which this study would be impossible.

8. REFERENCES

Armaly, B. F., Durst, F., Pereira, and J. C. F. & Schonung, B., 1983, “Experimental and Theoretical Investigation of Backward-Facing Step Flow”, Journal of Fluid Mechanics, Vol. 127, pp. 473-496.

Comini, G., Manzam, M. and Cortella, G., 1997, “Open Boundary Conditions for the Streamfunction-Vorticity Formulation of Unsteady Laminar Convection”, Numerical Heat Transfer, Part B, Vol. 31, pp. 217-234.

Fu, W.S., Cheng, C.S. and Shieh, W.J., 1994, “Enhancement of Natural Convection Heat Transfer of an Enclosure by a Rotating Circular Cylinder”, Int. J. Heat Mass Transfer, Vol. 37, No. 13, pp. 1885-1897.

Gartling, D. K., 1990, “A Test Problem for Outflow Boundary Conditions – Flow over a Backward-Facing Step”, International Journal of Numerical Methods in Fluids, Vol. 11, pp. 953-967.

Kim, J. and Moin, P., 1985, “Application of a Fractional-Step Method to Incompressible Navier-Stokes Equations”, Journal of Computational Physics, Vol. 59, pp. 308-323.

Lee, J., Kang, S. H. and Son, Y. S., 1999, “Experimental Study of Double-Diffusive Convection in a Rotating Annulus with Lateral Heating”, Int. J. Heat Mass Transfer, Vol. 42, pp. 821-832.

Lee, T. and Mateescu, D., 1998, “Experimental and Numerical Investigation of 2-D Backward-Facing Step Flow”, Journal of Fluids and Structures, Vol. 8, pp. 1469-1490.

Lin, D. and Yan, W.M., 2000, “Experimental Study of Unsteady Thermal Convection in Heated Rotating Inclined Cylinders”, Int. J. Heat Mass Transfer, Vol. 43, pp. 3359-3370.

Nguyen, H. D., Paik, S. and Douglass, R. W., 1996, “Unsteady Mixed Convection About a Rotating Circular Cylinder with Small Fluctuations in the Free-Stream Velocity”, Int. J. Heat Mass Transfer, Vol. 39, No. 3, pp. 511-525.

Sohn, J., 1998, “Evaluation of FIDAP on Some Classical Laminar and Turbulent Benchmarks”, International Journal of Numerical Methods in Fluids, Vol. 8, pp. 1469-1490.

Yoo, J., 1998, “Mixed Convection of Air Between Two Horizontal Concentric Cylinders with a Cooled Rotating Outer Cylinder”, Int. J. Heat Mass Transfer, Vol.41, No. 2, pp. 293-302.

9. RESPONSIBILITY NOTICE

The authors are the only responsible for the printed material included in this paper.